

HAAP: Vision-context Hierarchical Attention Autoregressive with Adaptive Permutation for Scene Text Recognition

Honghui Chen, Yuhang Qiu, Jiabao Wang, Pingping Chen, *Senior Member, IEEE*, and Nam Ling, *Life Fellow, IEEE*

arXiv:2405.09125v1 [cs.CV] 15 May 2024

Abstract—Internal Language Model (LM)-based methods use permutation language modeling (PLM) to solve the error correction caused by conditional independence in external LM-based methods. However, random permutations of human interference cause fit oscillations in the model training, and Iterative Refinement (IR) operation to improve multimodal information decoupling also introduces additional overhead. To address these issues, this paper proposes the Hierarchical Attention autoregressive Model with Adaptive Permutation (HAAP) to enhance the location-context-image interaction capability, improving autoregressive generalization with internal LM. First, we propose Implicit Permutation Neurons (IPN) to generate adaptive attention masks to dynamically exploit token dependencies. The adaptive masks increase the diversity of training data and prevent model dependency on a specific order. It reduces the training overhead of PLM while avoiding training fit oscillations. Second, we develop Cross-modal Hierarchical Attention mechanism (CHA) to couple context and image features. This processing establishes rich positional semantic dependencies between context and image while avoiding IR. Extensive experimental results show the proposed HAAP achieves state-of-the-art (SOTA) performance in terms of accuracy, complexity, and latency on several datasets.

Index Terms—Language models (LM), Autoregressive generalization, Multimodal information.

I. INTRODUCTION

SCENE Text Recognition (STR) aims to transcribe the text in an image into a computer-readable text format i.e., to recognize the localized text regions. Scene text with rich information plays a vital role in a range of applications such as visual quizzing, autonomous driving, image retrieval, augmented reality, retail, education, and visually impaired devices [1–5].

In contrast to Optical Character Recognition (OCR) in documents with more homogeneous text attributes, STR has to deal with irregular text, such as rotation, bending, blurring, or occlusion. In addition, noise and distortion issues make STR challenging. STR is primarily a visual task, involving two different modalities: image and text. Early work still

Honghui Chen, Jiabao Wang, Pingping Chen are with the College of Physics and Information Engineering, Fuzhou University, Fuzhou, 350108, China (e-mail: chh5840996@gmail.com; wabb0811@163.com; ppchen.xm@gmail.com).

Yuhang Qiu is with the Faculty of Engineering, Monash University, Clayton, VIC, 3800, Australia (e-mail: yuhang.qiu@monash.edu).

Nam Ling is with the Department of Computer Science and Engineering, Santa Clara University, Santa Clara, California, 95053, USA (e-mail: nling@scu.edu).

Manuscript received January 31, 2024.

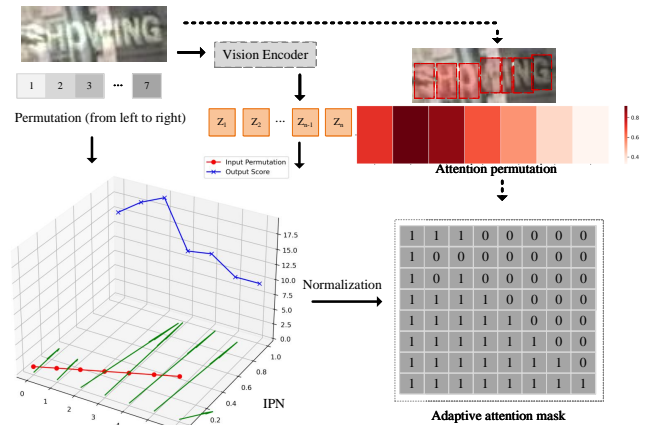


Fig. 1. Illustration of IPN. The solid line represents the process of mask generation i.e. non-linear weighted mapping of left-to-right permutations. The dashed line represents the interpretation of the mask generation: the visual information guides the adaptive mask to learn the inter-correlation of the contextual positions.

tends to rely on a backbone pre-trained on unimodal data. Learning from data [6–13] is achieved by combining visual features with semantic priors from word representation models [14] or dictionaries [15] as well as sequence modeling [16]. However, there are inherent limitations in models based on visual information. Visual features alone are not sufficient in cases where the text part is unreadable, e.g., occlusion. Additionally, STR is a One-shot task that has data independence. And, textual semantics can assist visual models in recognizing heterogeneous data.

Zhao et al. verified that language modeling (LM) can effectively focus on text and accurately determine the meaning of words [13]. LM demonstrates the special ability to perceive and understand text in natural images. For that, the combination of LM and visual models for sequence modeling is the current mainstream [8–13]. It is divided into two categories: external LM-based and internal LM-based. External LM-based schemes essentially accomplish STR by introducing external LMs to assist in correcting visual model reasoning [8–11]. External LM causes error correction own to the conditional independence of the input. The condition assumes that each pixel or character is independent, regardless of their interactions. However, the reality is that the order and spatial position of the characters about each other affect

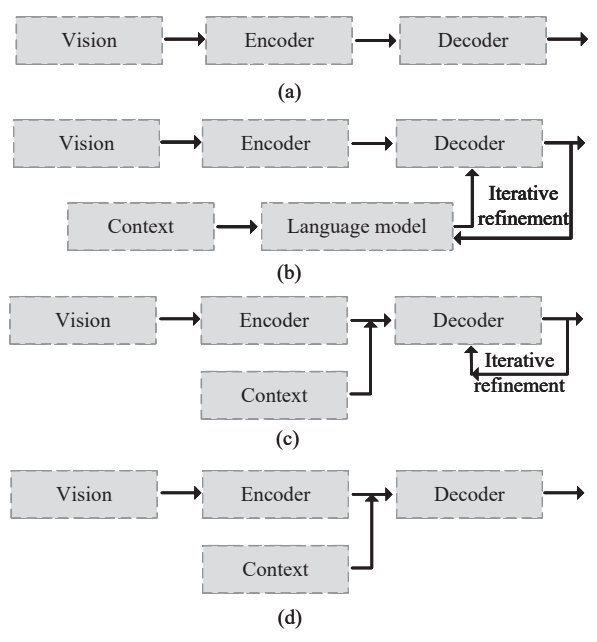


Fig. 2. The basic flow of STR. (a) Visual feature coding and decoding (b) Visual-contextual representation based on external LM. (c) Visual-contextual representation based on internal LM. (d) Internal LM-based visual-contextual representation without Iterative Refinement (IR) (Ours).

their meaning and grammatical structure. Algorithms that only consider each character by itself and ignore interactions can lead to prediction errors, especially when the input text has a complex structure and arrangement. Therefore, Permutation Language Modeling (PLM) is employed to improve the generalization of autoregressive (AR) modeling by parsing sequence meaning and syntactic structure [12, 13]. PLM models can be viewed as a collection of AR models with shared architecture and weights. Token dependencies are specified dynamically through the use of an attention mask. Although randomized permutation increases the diversity of data, this strategy is accompanied by training fit oscillations since the random subset has the uncertainty of human interference. We also find that random permutation leads to unstable convergence of the model during training. In addition, if the model only performs well for specific alignments, it leads to a degradation of the generalization performance. Next, recent approaches have used Transformer encoder-decoder based for cross-modal visual and semantic information fusion [8–13]. However, They need to optimize the predictions through additional Iterative Refinement (IR). Essentially, internal LM is introduced in the decoder can eliminate IR, which is only an additional decoding because the visual and LM are jointly parsed. Considering that noisy inputs still have errors from the output of the visual model, IR is proposed to refine predictions from visual and language cues in external LM-based scenarios. Therefore, recent internal LM-based schemes do not propose an efficient way to couple cross-modal information in the decoder but rely on additional IR.

This paper proposes the Hierarchical Attention AR Model with Adaptive Permutation (HAAP) to address these issues. The motivation is depicted. First, the use of an adaptive

permutation instead of a random permutation scheme increases the diversity of the training data and prevents dependence on a specific order. It reduces the training overhead of the PLM while avoiding training fitting oscillations (as shown in Fig. 1). Second, Multi-head Attention (MHA) is introduced to hierarchically couple cross-modal information. Hierarchical processing improves the adaptation of visual features to semantics and thus enhances end-to-end joint parsing without additional IR (as shown in Fig. 2).

First, inspired by traditional neurons and self-attentive mechanisms, this paper proposes an Implicit Permutation Neurons (IPN) to adapt the ordering between characters in the internal LM. The ordering and spatial location of the characters are considered rather than independently. IPN assigns a set of queries to the original left-to-right permutation to map it linearly into the high-dimensional space. Immediately, two sets of weight matrices are utilized for query weighting and inverse mapping. The process is still able to capture nonlinear relationships in the data with learnable weights. Second, this paper proposes Cross-modal Hierarchical Attention mechanism (CHA) to couple cross-modal information. Contexts embedded in the high dimensional space establish semantic dependencies through self-attention. The context interacts with the image features for the first time to context-image feature alignment. Next, the encoded location is matched with the context and then coupled with the image features again by mutual attention. Hierarchical feature processing drives the interactions of each item in the sequence while capturing the dependencies between locations using an image-guided context-assisted model. In addition, the location-context-image interaction is improved with location inter-correlation guided by adaptive mask and the uniform gradient flow. Therefore, the model avoids additional overhead by eliminating IR and achieves end-to-end parsing.

The contributions of this paper can be summarized as follows:

- This paper proposes an internal LM-based HAAP to unify end-to-end coupling of location coding, image features, and context to improve the generalization ability of the model in various STR scenes.
- We propose a novel neuronal structure i.e. IPN to capture the dependencies between characters via adaptive masks efficiently. The model automatically learns the optimal alignment form by capturing the nonlinear relationships during the learning of weights without manual design.
- We propose hierarchical feature processing CHA to motivate the interaction of each item in the sequence, together with adaptive masks to improve the location-context-image interaction.
- HAAP achieves state-of-the-art (SOTA) results on the STR benchmark for all character sets as well as on larger, more difficult real datasets that include occluded and arbitrarily oriented text (as shown in Table. II). Besides, HAAP also shows the cost-quality trade-offs in terms of parameters, FLOPs, and runtime usage (as shown in Table. IV).

The rest of the paper is structured as follows: section II

discusses related work. Section III describes the architecture of the proposed algorithm in detail. Section IV describes the experiments and analysis and the summary in Section V.

II. RELATED WORK

In this section, we review current deep learning-based STR methods. Recent studies are mainly categorized into two directions, context-independent and context-relevant, based on whether textual semantics are considered or not. We summarize and discuss the research in these two directions separately.

A. Context-independent STR

Considering that STR is essentially a visual task, the researchers intuitively represent the inputs by constructing a visual model based on deep learning. This is the context-independent scheme i.e., category inference by summarizing visual features. Further, context-independent STR can be categorized into parallel-based reasoning and sequential reasoning. The parallel-based scheme only uses the visual features for prediction without considering the relationship between characters. Its main application is Fully Convolutional Network (FCN) [17] to segment characters at the pixel level. Liao et al [18] recognized characters by grouping segmented pixels into text regions. Wan et al [19] proposed an additional sequential segmentation map that records characters in the correct order. Multi-category classification is unable to accurately construct complete phrases because the output characters are conditionally uncorrelated with each other.

Immediately, the scheme of sequence inference using Recurrent Convolutional Networks (RNN) was proposed to capture the correlation of characters [20]. The most typical is the Connectionist Temporal Classification (CTC) [21] based scheme. The RNN models the sequential sequence of features extracted by a convolutional neural network (CNN) and is trained end-to-end using CTC loss [22]. The RNN receives the current input and the previous hidden state at each time step and outputs the current hidden state. This sequential modeling structure allows the RNN to naturally adapt to the characteristics of sequential data, to parse the syntactic and semantic structures in the text. RNN is also used in a series of Attention-based [23] schemes. Several attempts have explored the enhancement of image encoding and decoding by employing different attentional mechanisms [24–26]. Character classification by aligning features and character positions, or converting STR into a multi-instance learning problem [7, 27]. Sequence modeling was given a new lease of life with the introduction of transformer [16, 28]. Transformer was then proposed as an alternative to RNN for sequence modeling [29–35]. However, context-independent methods that rely only on image features for prediction cannot address recognition in low-quality images, especially being less robust to corruption such as occlusion, distortion, or incomplete characters. This limitation motivates the use of language semantics to make recognition models more robust.

B. Context-relevant STR

Context-dependent STR is a typical cross-modal fusion scenario since the internal interactions between vision and language are constructed. Considering that textual semantics can assist visual models in processing heterogeneous data, the community has recently appeared with a large number of researches to assist recognition by constructing LMs [8–14, 36]. VisionLAN [8] introduced character masking to guide the visual model to refer to language information in the visual context. MATRN [10] referenced context to enhance visual and semantic features based on spatial coding. STRT [11] designed an iterative text Transformer to predict the probability distribution in a sequence of characters. It is shown that robust models can be constructed by introducing external LMs for explicit modeling. Considering that character sequences are usually modeled in a left-to-right manner, the researcher develops the integrated model to capture twice the amount of information through the bi-directional LM [6, 7, 37, 38]. SRN [7] combined the features of two unidirectional Transformers for prediction, which resulted in twice as expensive both computationally and parametrically. Therefore, ABINet [9] used a novel bidirectional completion network based on bidirectional feature representation. However, the conditional independence of external LM on image features limits its performance and makes error corrections. Subsequently, the internal LM was re-proposed for implicit language modeling to improve visual-contextual interaction. PARSeq [12] used PLM rather than standard AR modeling to learn internal LMs. It supports flexible decoding by using a parameterization that decouples the decoding location from the input context. CLIP4STR [13] introduced an encoder-decoder to process image and text information. The encoder is inherited from CLIP [39], while the decoder uses Transformer.

Internal LR-based schemes mitigate the problem of noisy inputs as well as increase the diversity of the data by dynamically specifying the sequence order through the use of an attention mask. However, the strategy of using randomized permutations introduces training fitting oscillations due to the uncertainty of randomized permutations with human interference. Furthermore, most of these context-dependent STR models use Transformer-based encoder-decoders to implement with IR. However, internal LM-based schemes rely on IR to address noisy inputs in external LM-based models. Thus, the decoding strategy of LM model-based schemes at this stage is inefficient and introduces additional computational effort. This paper proposes to use an adaptive sequence ordering scheme to increase the diversity of the training data and prevent the dependence of the model on a specific order. To further enhance the efficiency of cross-modal information coupling at the decoder side, MHA is developed to Hierarchical coupling information, improving the semantic adaptation of visual features. Ultimately, end-to-end joint parsing is enhanced to avoid additional IR.

III. METHODOLOGY

In this section, we present in detail the principles and framework of our proposed Hierarchical Attention AR Model

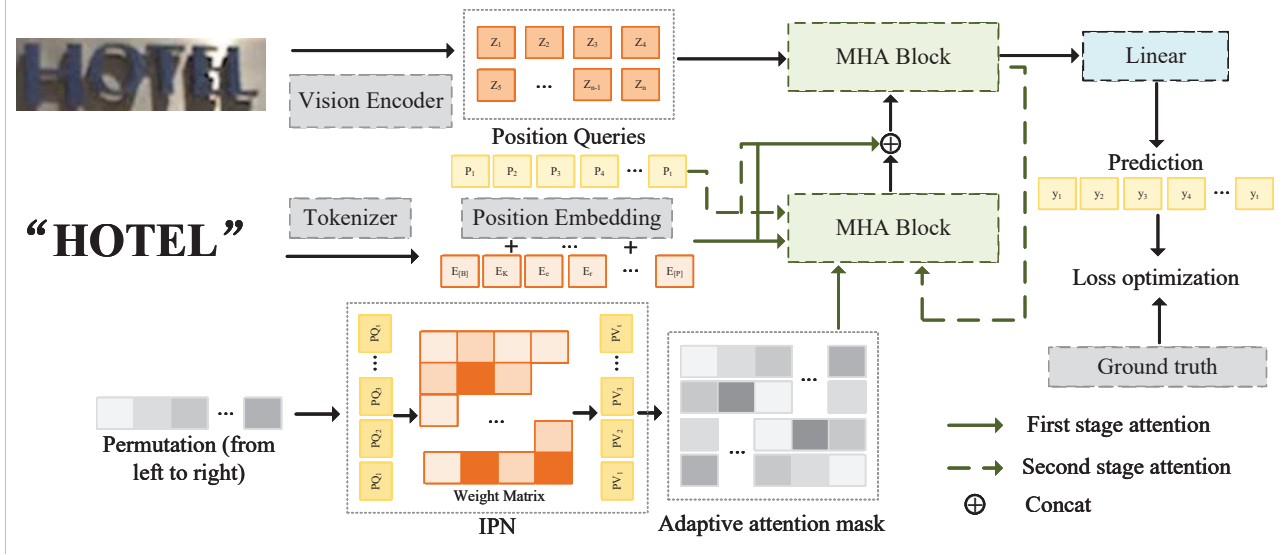


Fig. 3. The pipeline of HAAP. (a) Image and text inputs are represented as a series of patches and semantic tokens. (b) Visual information guides the IPN to assign bidirectional and adaptive masks to the context. (c) MHA is used to perform hierarchical image-context interaction and decoding.

with Adaptive Permutation (HAAP), including Implicit Permutation Neurons (IPN) and Cross-modal Hierarchical Attention mechanism (CHA).

A. Overview

HAAP follows an encoder-decoder architecture as shown in Fig. 3. In the encoding phase, the image and text inputs are represented as a series of patches and semantic tokens. Subsequently, MHA is used for hierarchical image-context interaction and decoding. Specifically, first, the Transformer encoder [28] is utilized to establish the internal feature associations of the image patches. Second, the IPN assigns bi-directional and adaptive permutation masks to the textual context for adjusting sequence order. The contexts embedded into the high-dimensional features are first established by self-attention to establish internal associations. Then MHA is used for context and visual information interaction and position query association. Third, the associated information further interacts with the visual information by utilizing mutual attention. Next, the position query is linearly decoded into contextual output.

B. Encoder

Vision encoder Considering that ViT [28] divides images into patches and uses full connectivity to learn global relationships can better extract global and complex visual information than traditional CNNs [40], HAAP follows the original ViT structure to build the visual encoder, which consists of $L = 12$ layers of Transformer encoder. All layers share the same architecture as shown in Fig. 4. The output of the last encoder is subjected to a Layer Normalization (LN). Formally, first, the image of size $H \times W \times C$ (height H , width W , channels C) is reshaped into a series of flat 2D patches $x_p \in \mathbb{R}^{N \times (P^2 - C)}$, where (P, P) is the resolution of each image block and $N = HW/P^2$ is the number of blocks generated. The patch

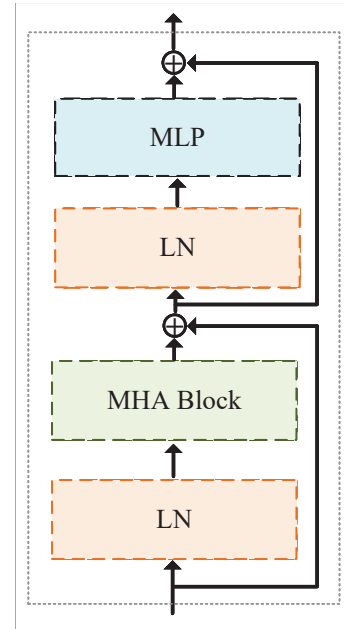


Fig. 4. Illustration of a ViT layer from Dosovitskiy et al. [28]. LN pertains to layer normalization. MLP represents Multilayer Perceptron.

x_p is flattened and mapped to D dimensions using a trainable linear projection $E \in \mathbb{R}^{(P^2 C) \times D}$. The position embedding $E_{pos} \in \mathbb{R}^{(N+1) \times D}$ is added to the projected output z , as:

$$z = [x_p^0 E; x_p^1 E; x_p^2 E; \dots; x_p^N E;] + E_{pos}, \quad (1)$$

where x_p^i represents the i -th x_p . z performs feature extraction in alternating MHA and Multi-Layer Perceptron (MLP). A normalized LN is applied initially in each block to mitigate internal covariate bias during training. Additionally, residual concatenation is applied twice in the block to aid gradient propagation in the depth model, as:

$$z'_l = MHA(LN(z_{l-1})) + z_{l-1}, l \in [1, L] \quad (2)$$

$$z_l = MLP(LN(z'_l)) + z'_l, l \in [1, L] \quad (3)$$

where MLP contains two nonlinear layers with GELU activation functions. The z'_l and z_l are the visually encoded information. MHA is the extension of scaled dot-product attention to multiple representation subspaces or heads. In scaled dot-product attention, the similarity scores are computed using dot-product computation of the similarity between two d_k -dimensional vectors query q , and key k . Attention scores are transformed by the d_v -dimensional vector values v . The scaled dot product attention is defined as:

$$Attn(q, k, v) = softmax\left(\frac{qk^T}{\sqrt{d_k}}\right)v, \quad (4)$$

further,

$$MHA(q, k, v) = Concat(head_1, \dots, head_h)W^o, \quad (5)$$

where

$$head_i = Attn(qW_i^q, kW_i^k, vW_i^v), \quad (6)$$

where the computational cost of MHA is practically constant due to the dimension of the vector $d_{head} = d_{model}/h$, where h is the number of heads. The $W^q, W^k, W^v \in \mathbb{R}^{d_{model} \times d_{head}}$ are obtained by connecting the heads and multiplying with the output projection matrix $W^o \in \mathbb{R}^{d_{model} \times d_{head}}$.

Context encoder The context uses a Tokenizer [12] for lowercase byte pair encoding BPE. The start, padding, and end of the text sequence are padded with [SOS], [PAD] and [EOS] tokens, respectively.

C. Implicit Permutation Neurons (IPN)

Considering that STR traditionally relies on left-to-right $P_{left2right}$ or right-to-left $P_{right2left}$ unidirectional sequence modeling, we propose IPN to improve the correlation between inputs and outputs through multidirectional sequence modeling. Essentially, multidirectional sequence modeling considers internal correlations while considering bi-directionality to avoid the effects of word syntactic structures or external disturbances such as occlusions and distortions. For example, to predict the "e" in the word "clearance", we consider "cl_" and "ecnara_." in the context of "cl_ar". IPN provides an attention mask during the attention operation to generate dependencies between the input context and the output without actually replacing the text labels. Table. I illustrates three examples of the mask.

Formally, first, given the T -length text labels $y = [y^1, y^2, \dots, y^T]$, decompose the likelihood $[1, 2, \dots, T]$ according to the canonical order using the chain rule to build a left-to-right permutation of $P_{left2right}$ to obtain the model inference as:

$$\log p(y|x) = \sum_{t=1}^T \log p_\theta(y_t | y_{<t}, x), \quad (7)$$

where θ represents the model parameter and x is the input image. Second, to learn and extract complex structural properties from the data, P_{query} is assigned to T positions in

TABLE I
ILLUSTRATION OF MASKS FROM IPN. $P_{left2right}$ AND $P_{right2left}$ REPRESENT THE LEFT-TO-RIGHT AND RIGHT-TO-LEFT PERMUTATION. [B] AND [E] REPRESENT THE BEGINNING AND END OF THE SEQUENCE. $y1, y2, y3$ REPRESENT THE THREE POSITIONS OF THIS SEQUENCE. 1 INDICATES THAT THE OUTPUT HAS A CONDITIONAL DEPENDENCY ON THE INPUT. 0 INDICATES THAT THERE IS NO INFORMATION FLOWING FROM INPUT TO OUTPUT.

$P_{left2right}$		Mask		
	[B]	y1	y2	y3
y1	1	0	0	0
y2	1	1	0	0
y3	1	1	1	0
[E]	1	1	1	1

$P_{right2left}$		Mask		
	[B]	y1	y2	y3
y1	1	0	1	1
y2	1	0	0	1
y3	1	0	0	0
[E]	1	1	1	1

Attention mask of IPN				
	[B]	y1	y2	y3
y1	1	0	1	1
y2	1	1	0	0
y3	1	1	1	0
[E]	1	1	1	1

the $P_{left2right}$ sequence and projected to a high-dimensional space, as:

$$M_t = P_{left2right}^T \cdot P_{query}, \quad (8)$$

where $M_t \in \mathbb{R}_T^T$ represents the intermediate matrix.

Third, the model learns the optimal representation without manually designing features via a learnable weight matrix P_{weight} , as:

$$M_w = M_t \cdot P_{weight}, \quad (9)$$

where M_w is the weighted transformation matrix. This process helps the model to parse the representation of the structure of the input data. Even though there is no explicit nonlinear activation function throughout the process, the model is still able to capture the nonlinear relationships in the data because of the learning of the weights. Fourth, the transformation matrix is inversely mapped to the sequence of scores P_{score} via P_{value} , as:

$$P_{score} = M_w \cdot P_{value}^T. \quad (10)$$

Next, P_{score} is normalized from largest to smallest to generate the actual ranking order. Immediately, we invert the left-to-right permutations $[1, 2, \dots, T]$ and invert the adaptive permutation pairs to obtain twice the amount of information.

D. Cross-modal Hierarchical Attention mechanism (CHA)

The standard Transformer parametric AR model is inefficient for decoding in multidirectional sequence modeling since the feature distribution predicted by the hidden state is independent of the target location [41]. Let us assume that we parameterize the next token distribution as:

$$p_\theta(x_{rt} = x | x_{r<t}) = \frac{\exp(e(x)^T h_\theta(x_{r<t}))}{\sum x' \exp(e(x')^T h_\theta(x_{r<t}))}, \quad (11)$$

where $h_\theta(x_{r<t})$ denotes the hidden representation of $x_{r<t}$ produced by the shared transformer network after proper masking. We use rt and $r < t$ to denote the t -th and the first $t - 1$ elements of the permutation set r . Since the same model parameter θ is shared between all decomposition sequences during training, rt is expected to see that every possible element in the sequence is not equal to x_t . Note that the representation $h_\theta(x_{z<t})$ does not depend on the position it will predict, i.e. the value of rt . Two different target positions share the same model predictions. However, the ground truth distributions for the two positions are certainly different.

To avoid this problem, we perform context and location encoding based on a two-stream attention mechanism to provide complete contextual information. We use two sets of hidden representations i.e., from content and query representations. Meanwhile, considering that context and location need to interact with visual features cross-modally for alignment, we adopt a hierarchical coupling approach, i.e., CHA, to consider the context-location-image association. In the first stage, context-visual attention is established after self-attentive encoding of sorted contexts, as:

$$Attn_{cv} = p + dropout[MHA(Attn_c, z)], \quad (12)$$

where

$$Attn_c = c + dropout[MHA(c, c, M)], \quad (13)$$

where $c \in \mathbb{R}^{(T+1) \times d_{model}}$ is the contextual embedding with positional information and $M \in \mathbb{R}^{(T+1) \times (T+1)}$ is the attention mask. The total sequence length is increased to $T + 1$ by using special separator markers.

Next, MHA is used to establish positional-contextual-visual attention, as:

$$Attn_f = Attn_p + dropout[MHA(Attn_p, z)], \quad (14)$$

where

$$Attn_p = p + dropout[MHA(p, Attn_{cv}, M)]. \quad (15)$$

The strategy of hierarchical feature processing prompts sequence interactions while utilizing image-guided context to assist the model in capturing dependencies between locations. The location-context-image interaction capability is boosted since adaptive permutation guides location interconnections. The robustness of the model is improved because the uniform gradient flow allows them to interact with each other during training. Finally, the output logits y' are obtained as:

$$y' = Linear(Attn_f) \in R^{(T+1)(S+1)}, \quad (16)$$

where S is the size of the character set used for training. Additional characters are associated with the [E] tag (the end of the tagging sequence). The complete training loss for the optimization phase is the average of the K cross-entropy loss \mathcal{L}_{ce} with attention mask, as:

$$\mathcal{L} = \frac{1}{k} \sum_{k=1}^K \mathcal{L}_{ce}(y'_k, y), \quad (17)$$

where y'_k represents the k -th output logit and y is the real label. $K = 4$ is the number of permutations.

IV. EXPERIMENTS

A. Dataset

This experiment uses both synthetic training datasets MJSynth (MJ) [27] and SynthText (ST) [42] as well as real data for training including nine real-world datasets (COCO-Text (COCO) [43], RCTW17 [44], Uber-Text (Uber) [45], ArT [46], LSVT [47], MLT19 [48], ReCTS [49], TextOCR [50] and OpenVINO [51]). We use IIIT 5k-word (IIIT5k) [52], CUTE80 (CUTE) [53], Street View Text (SVT) [54], SVT-Perspective (SVTP) [55], ICDAR 2013 (IC13) [56] and ICDAR 2015 (IC15) [57], COCO, Uber, ArT for testing. The dataset contains challenging texts such as multi-orientation, curvature, perspective blur, low resolution, distortion, and occlusion.

Synthetic datasets MJ consists of 8.9 million photorealistic text images composed of artificial datasets through over 90k English dictionaries. The composition of MJ consists of three parts background, foreground, and optional shadow/border respectively. It uses 1400 different fonts. Additionally, the font word spacing, thickness, underlining, and other attributes of MJ are different. MJ also utilizes different background effects, border/shadow rendering, base shading, projection distortion, natural image blending, and noise. ST consists of 8 million word text images synthesized by blending text over natural images. It uses scene geometry, textures, and surface normals to naturally blend and distort text renderings on the surfaces of objects in the image. Similar to MJ, ST uses randomized fonts for its text. The text image is cropped from the natural image in which the synthesized text is embedded.

Real-world datasets The COCO dataset has a total of 73,127 training and 9.8k test images containing non-text, legible text, illegible text, and occluded text images. Each image contains at least one instance of legible text. RCTW contains 12,263 annotated images of the large-scale Chinese field dataset. The Uber dataset has a total of 127,920 training 60,000 test images collected from Bing Maps Streetside. It contains house numbers and vertical and rotated text on sign boards. The ArT dataset was created to recognize arbitrarily shaped text containing 32,028 training and 26,000 testing images of perspective, rotated, or curved arbitrarily shaped text. SVT is a large-scale street scene text dataset collected from streets in China totaling 41,439 text images of arbitrarily shaped natural scenes. MLT19 was created to recognize multilingual text. It has a total of 56,727 training images consisting of seven languages: Arabic, Latin, Chinese, Japanese, Korean, Bengali and Hindi. The ReCTS dataset contains 26,432 irregular texts arranged in various layouts or written in unique fonts. TextOCR and OpenVINO are large datasets with very diverse images containing 818,087 and 2,071,541 images respectively. They have complex scenes with multiple objects and text of different resolutions, orientations, and qualities.

The IIIT5k dataset is a collection of 5000 natural scene and digitally born text images crawled from Google image search

containing 2,000 images for evaluation and 3,000 images for testing. It has low resolution, multiple font styles, light and dark transformations, and projection distortion. CUTE contains 288 cropped images for the curved text collection. The images were captured by digital cameras or collected from the Internet. SVT is a collection of street view text from Google Street View. It contains 257 images for evaluation and 647 images for testing. Further, the SVTP dataset is a more complex collection of images containing numerous perspective texts totaling 645 images for testing. IC13 and IC15 were created for the ICDAR Robust Reading Contest. IC13 contains 848 images for training and 1,015 images for evaluation. IC15 contains 4,468 images for training and 2,077 images for evaluation. Many of the samples contain perspective, and blurred text.

B. Implementation Details

The entire training and testing is implemented in two RTX 3090 GPUs with 24GB of RAM based on the Pytorch library [59]. The training is performed with a batch size of 1024 for 63,630 iterations i.e. 20 epochs on a real dataset of 3,257,585 samples and 4 epochs on a synthetic dataset of 16.89M samples. Following previous work [12], the Adam [60] optimizer is used along with the 1cycle [61] learning rate scheduler with an initial learning rate of $7e - 5$. We set a maximum label length of $T = 25$ and used a character set of size $S = 94$ containing mixed-case alphanumeric characters and punctuation. The image is enhanced, resized, and normalized. First, the image enhancement is done using a three-layer RandAugment [62] operation where sharpening is tuned to Gaussian Blur and Poisson Noise. Second, the image is unconditionally resized to 128×32 pixels, and patches of 8×4 size are used. For the model testing phase, we use a 36-character set i.e. containing numbers and 26 letters. We use word accuracy as the main evaluation metric i.e., the prediction is considered correct if and only if the characters match at all positions.

Remark The highlighted red and red lines in the visualization results indicate error recognition and omissions, respectively. The best performance result is shown in bold font.

C. Comparison with State-of-the-Arts

We compare HAAP with recent methods on 6 public benchmarks, and the quantitative results are listed in Table. II. We can see that HAAP outperforms the benchmark Parseq [12], realizing SOTA performance. The recognition performance in IC15 (incident scene text), SVTP (perspective scene text), and CUTE80 (curved text line image) are improved by 1.1%, 1.7%, and 1% respectively. Our model achieves 99.3% recognition accuracy on the IIIT5K (distorted, low-resolution scene text) dataset. This is an improvement of 2.6% compared to the latest method, HVSI [35]. This verifies the excellent performance of HAAP on irregular text datasets, which contain a large number of low-quality images such as noisy and blurred images.

Besides validating the model on small-scale public benchmarks, we evaluate HAAP on three larger and more challenging recent benchmarks consisting of irregular text with different shapes, low-resolution images, rotations, and occlusions. The results are shown in Table. III. It achieves 80.6%, 85.5%, and 85.8% outperforms the previous methods in terms of accuracy, respectively. Representative visible results are shown in Fig. 6, which demonstrates that our method is sufficiently robust to occlusion and text direction variability. In detail, we find that HAAP and recent methods are effective in solving complex background problems caused by perspective shifts or uneven lighting. However, artistic lettering and occlusion can lead to errors in previous work. The independence of heterogeneous data leads to ambiguous judgments by the recognizer, which can be effectively avoided by HAAP. Furthermore, HAAP can protect against additional distortions and ambiguities. For example, although the second half of "CORNER" in Fig. 6 is ambiguous, our model can still reason effectively. HAAP also recognizes that the "R" in "SHARP" in Fig. 6 relies on AR reasoning with adaptive permutations.

TABLE III
THE COMPARISON OF WORD ACCURACY ON THREE CHALLENGING DATASETS. "S" AND "R" DENOTE SYNTHETIC AND REAL DATA, RESPECTIVELY.

Method	Train data	COCO	ArT	Uber
CRNN(2016)[22]	S	49.3	57.3	33.1
TRBA(2021)[30]	S	61.4	68.2	38.0
ViTSTR(2021)[29]	S	56.4	66.1	37.6
ABINet(2021)[9]	S	57.1	65.4	34.9
PARSeq(2022)[12]	S	64.0	70.7	42.0
HAAP	S	65.0	71.7	43.2
CRNN(2016)[22]	R	62.2	66.8	51.0
TRBA(2021)[30]	R	77.5	82.5	81.2
ViTSTR(2021)[29]	R	73.6	81.0	78.2
ABINet(2021)[9]	R	76.5	81.2	71.2
PARSeq(2022)[12]	R	79.8	84.5	84.1
HAAP	R	80.6	85.5	85.8

In addition, Fig. 5 and Table. IV shows the trade-off between accuracy and cost (parameters, FLOPS, and latency). For concise representation, we use *Avg* to denote the average accuracy, which is computed as a weighted average based on the number of datasets. HAAP achieves the highest average word accuracy and exhibits competitive cost quality in all three metrics. Compared to PARSeq, HAAP uses far fewer parameters and FLOPs. In terms of latency, HAAP achieves *Avg - 6* of 95.0% with 15.2 ms/image, which outperforms previous methods.

TABLE IV
COMPARISON WITH OTHER METHODS IN TERMS OF COMPLEXITY AND EFFICIENCY. *AVG - 6* REPRESENTS THE AVERAGE ACCURACY IN THE SIX BENCHMARKS.

Method	Parameters(M)	Flops(G)	Latency(ms)	Avg-6(%)
TRBA[30]	49.6	10.9	13.0	84.0
ABINet[9]	36.9	7.3	33.9	93.7
ViTSTR[29]	85.8	17.6	9.8	85.2
XIA et. al.[34]	87.2	12.6	37.6	88.4
PARSeq[12]	23.8	6.3	17.5	94.0
STRT[11]	57.9	20.6	31.8	92.8
Ours	23.8	3.2	15.2	95.0

TABLE II

THE COMPARISON OF WORD ACCURACY ON SIX COMMON BENCHMARKS IN TERMS OF BOTH CONTEXT RELEVANT AND INDEPENDENT. ‘‘S’’ AND ‘‘R’’ DENOTE SYNTHETIC AND REAL DATA, RESPECTIVELY.

Method	Train data	IIIT5K(%)	SVT(%)	IC13(%)	IC13(%)	IC15(%)	IC15(%)	SVTP(%)	CUTE(%)
Context-independent									
CRNN(2016)[22]	S	84.3	78.9	–	88.8	–	61.5	64.8	61.3
SRN(2020)[7]	S	94.8	91.5	95.5	–	82.7	–	85.1	87.8
ViTSTR(2021)[29]	S	88.4	87.7	93.2	92.4	78.5	72.6	81.8	81.3
TRBA(2021)[30]	S	92.1	88.9	–	93.1	–	74.7	79.5	78.2
TRAN(2023)[31]	S	94.3	90.7	–	93.6	–	77.7	85.0	81.6
DRNet(2023)[32]	S	93.4	90.6	–	95.8	–	81.6	83.6	83.0
CASR-DRNet(2023)[58]	S	95.1	92.3	–	95.3	–	83.0	85.0	89.2
I2C2W(2023)[33]	S	94.3	91.7	–	95.0	–	82.8	83.7	93.1
Xia et. al.(2023)[34]	S	91.9	91.3	96.1	94.2	80.6	78.0	83.4	88.8
HVSI(2024)[35]	S	96.7	94.9	–	97.4	–	86.2	89.2	95.5
Context-relevant									
SEED(2020)[14]	S	93.8	89.6	–	92.8	–	80.0	81.4	83.6
VisionLAN(2021)[8]	S	95.8	91.7	–	95.7	–	83.7	86.0	88.5
ABINet(2021)[9]	S	96.2	93.5	97.4	–	86.0	–	89.3	89.2
ABINet(2021)[9]	R	98.6	98.2	98.0	97.8	90.5	88.7	94.1	97.2
ConCLR(2022)[36]	S	96.5	94.3	–	97.7	–	85.4	89.3	91.3
MATRn(2022)[10]	S	96.6	95.0	97.9	95.8	86.6	82.8	90.6	93.5
PARSeq(2022)[12]	S	97.0	93.6	97.0	96.2	86.5	82.9	88.9	92.2
PARSeq(2022)[12]	R	99.1	97.9	98.3	98.4	90.7	89.6	95.7	98.3
STRT(2023)[11]	S	97.6	95.7	–	97.6	–	86.7	90.1	94.9
HAAP	S	97.7	95.1	97.2	96.4	87.8	85.6	90.7	95.1
HAAP	R	99.3	98.2	98.7	98.8	91.3	90.7	97.4	99.3

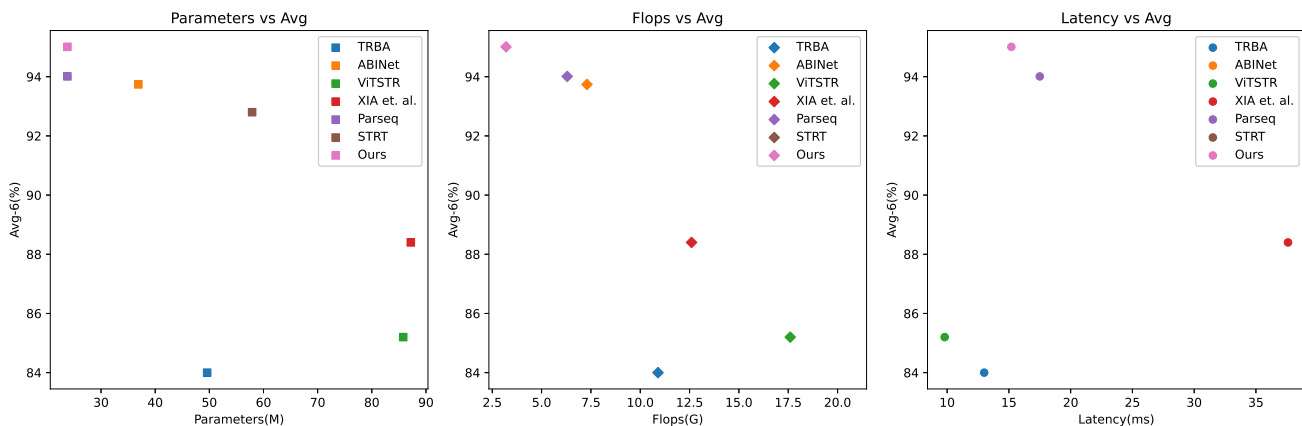


Fig. 5. Visual comparison with other methods in terms of complexity and efficiency.

D. Ablation study

To evaluate the effectiveness of the proposed HAAP with IPN and CHA, we conduct ablation studies on nine benchmark datasets. In these experiments, all models are trained using real datasets with consistent settings of their model hyper-parameters.

The effectiveness of IPN To study the impact of adaptive permutations generated by IPN, we compare the sequence modeling strategies using left-to-right, bi-directional, and PLM. From Table. V, we find that the model using the bidirectional can achieve about 3.4% improvement in $Avg - 9$ compared to the left-to-right strategy. This proves that the double amount of information brought by bidirectional sequence modeling can effectively improve the correlation ability between sequence contexts. The introduction of PLM allows the model to achieve 90.12% performance in terms of $Avg - 9$ along with an additional 4 sets of random permutations. Immediately, the model with IPN achieves 0.28%

performance gain in terms of $Avg - 9$ compared to the model with PLM. Meanwhile, as shown in Fig. 7, the model with IPN outperforms the introduction of PLM in terms of stability. This indicates that adaptive multi-directional sequence modeling can avoid the effects caused by the grammatical structure of words or by external disturbances. It also prevents uncertainty with human interference. The Comparison of qualitative results is shown in Fig. 8.

TABLE V
ABLATION STUDY OF THE IPN. $Avg - 9$ REPRESENTS THE AVERAGE ACCURACY IN NINE DATASETS. $P_{left2right}$ AND $P_{right2left}$ REPRESENT THE LEFT-TO-RIGHT AND RIGHT-TO-LEFT PERMUTATION.

$P_{left2right}$	$P_{right2left}$	PLM	IPN	Avg-9(%)
✓	-	-	-	86.63
✓	✓	-	-	89.99
-	-	✓	-	90.12
-	-	-	✓	90.40

	Ground truth	Ours	PARSeq [12]	ABINet [9]	ViTSTR [29]	CRNN [22]
	TEMT	TEMT	TENT	TENT	TENT	TENT
	FAMILY	FAMILY	FAMILY	FAMILY	FAM_UY	FAM_UV
	CORNER	CORNER	CORNES	CO_MER	CORNEL	CORNOL
	SHARP	SHARP	SHAPP	SHAPP	SHAPP	SHAPP
	PLACE	PLACE	P_APE	1009	SPAIBEE	AOE
	STHES	STHES	BERTIES	BAATES	GATTIE	SAL_ES
	LITTLE	LITTLE	LIM	LUN	LUN	AM
	VANILLA	VANILLA	VANILLA	VANILLA	VA_MLLA	VONILLO
	JEROME	JEROME	JLBOME	JLBOME	JEROME	ALBOHE
	6601	6601	5601	5601	5681	5607
	1605	1605	1805	1805	180	140

Fig. 6. Comparison of qualitative results on challenging textual data including blurring, distortion, occlusion, low resolution, perspective-shifting, and multi-directionality.

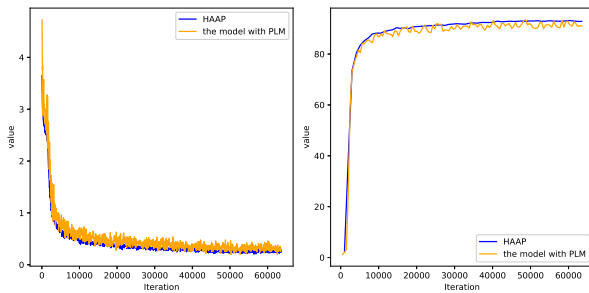


Fig. 7. Comparison of Loss (Left) and Valuation (Right) curves with IPN or PLM.

The effectiveness of CHA Considering that the unified gradient flow allows the modules to interact with each other, we evaluate CHA and MHA while evaluating their impact in different sequencing sequences. As shown in Table. VI, we find that the model with joint PLM and MHA (PLM+MHA) requires additional IR to improve the generalization. The PLM+CHA model achieves 90.15% performance in terms of *Avg* without additional IR, outperforming the performance of the PLM+MHA model with 3 number of refinement iterations (90.12%). In addition, compared to the PLM+MHA model, the IPN+CHA model achieves a performance gain of 0.59% without the need for refinement iterations. Besides, we find that the contribution of IR is minimal by introducing CHA in any sequence modeling (PLM or IPN). Because of the uniform gradient flow, the IPN+CHA model achieves the performance of 90.40% and gets a performance gain of 0.25% compared to the PLM+CHA model. This suggests that CHA can enhance the model generalization by providing effective positive feedback to the adaptive permutation.

	Ground truth	IPN	PLM	Bi-directional
	CANDY	CANDY	CANOY	CAMDY
	BRITISH	BRITISH	BRITISR	BRITISR
	GEMBIRA	GEMBIRA	GBMBIRA	GBMBIRA
	FANTASY	FANTASY	FONTASY	FNNTASV

Fig. 8. The qualitative results of the IPN.

TABLE VI
THE ABLATION STUDY OF CHA.

PLM	IPN	MHA	CHA	number of IR (Avg-9.(%))		
				0	1	2
✓	-	✓	-	89.81	89.96	90.12
✓	-	-	✓	90.15	90.17	90.15
-	✓	✓	-	89.97	90.21	90.28
-	✓	-	✓	90.40	90.43	90.42

The qualitative results of IPN and CHA are shown in Fig. 9. We find that the introduction of IPN and CHA makes the model not only effective for arbitrary orientation character recognition but also has strong generalization ability for low-quality and occlusion.

	Ground truth	IPN+CHA	IPN+MHA	PLM+CHA
	MARRIOTT	MARRIOTT	MO_M_OTT	MAMN_OTI
	23RDAV	23RDAV	23ROAV	23RONAV
	ITALIAN	ITALIAN	NALIAN	NALLAN
	CELEBRATING	CELEBRATING	GELEBRAZIME	GELELIATING

Fig. 9. Comparison of qualitative results.

E. Limitation and discussion

Although the proposed method can accurately recognize complex texts of arbitrary shapes in most cases, it still struggles with four kinds of tiny texts (image pixels not exceeding 2000): i:) front and back view severely confused; ii:) front and back text sticking together caused by blurring over long distances; iii:) shape-shifting with multiple occlusions; and iv:) alternating overlapping. Fig. 10 shows examples of such failure cases. The model loses attention on details during learning as the representation of character features declines in sequences.

Ground truth	Ours	PARSeq [12]	ABINet [9]	VITSTR [29]	CRNN [22]	
	6615	661_	662_	505_	661_	563_
	TEA	ARV	ART	ARV	ART	LV_
	chocolate	_acolate	_colate	_colote	_colote	_mlote
	MUSTANGS	MUSTANOS	MUST_NO_	MUSI_NUS	MUST_NIC	MUST_NIS
	LOCCITANE	OSPSA	DURNEY	STST	DER	MAEY

Fig. 10. Visualization results of some failure cases.

V. CONCLUSION

To improve the autoregressive generalization based on internal LM, this paper proposes HAAP to enhance the location-context-image interaction capability by designing IPN and CHA. First, IPN is used to parse sequence meaning and syntactic structure by dynamically specifying token dependencies with an adaptive attention mask. The adaptive AR subset increases the diversity of the training data and prevents model dependency on specific sequences. The training overhead of PLM can be reduced and training fitting oscillations is avoided. Second, CHA module for hierarchical feature processing is proposed to exploit position-context-image semantic dependencies in the sequence without IR. The experimental results validate the effectiveness and the SOTA performance of HAAP in terms of accuracy, complexity, and latency. In the future, we expect to extend HAAP to end-to-end detection and recognition, where the detector can be embedded in the visual decoder since the strong region perception is exhibited using the self-attention mechanism.

ACKNOWLEDGMENT

This work was supported by the Natural Science Fund of China under Grants 62171135, Industry-University Research Project of Education Department 2022.

REFERENCES

[1] H. Song, L. Dong, W.-N. Zhang, T. Liu, and F. Wei, "Clip models are few-shot learners: Empirical studies on vqa and visual entailment," *arXiv preprint arXiv:2203.07190*, 2022.
 [2] Y. Taki and E. Zemmouri, "Scene text recognition for text-based traffic signs," in *Advances in Intelligent Traffic and Transportation Systems*. IOS Press, 2023, pp. 67–77.
 [3] H. Luo, L. Ji, M. Zhong, Y. Chen, W. Lei, N. Duan, and T. Li, "Clip4clip: An empirical study of clip for end to end video clip retrieval and captioning," *Neurocomputing*, vol. 508, pp. 293–304, 2022.

[4] Z. Chen, F. Yin, Q. Yang, and C.-L. Liu, "Cross-lingual text image recognition via multi-hierarchy cross-modal mimic," *IEEE Transactions on Multimedia*, vol. 25, pp. 4830–4841, 2023.
 [5] Z. Li, X. Wang, Y. Liu, L. Jin, Y. Huang, and K. Ding, "Improving handwritten mathematical expression recognition via similar symbol distinguishing," *IEEE Transactions on Multimedia*, vol. 26, pp. 90–102, 2024.
 [6] B. Shi, M. Yang, X. Wang, P. Lyu, C. Yao, and X. Bai, "Aster: An attentional scene text recognizer with flexible rectification," *IEEE transactions on pattern analysis and machine intelligence*, vol. 41, no. 9, pp. 2035–2048, 2018.
 [7] D. Yu, X. Li, C. Zhang, T. Liu, J. Han, J. Liu, and E. Ding, "Towards accurate scene text recognition with semantic reasoning networks," in *Proceedings of the IEEE/CVF conference on computer vision and pattern recognition*, 2020, pp. 12 113–12 122.
 [8] Y. Wang, H. Xie, S. Fang, J. Wang, S. Zhu, and Y. Zhang, "From two to one: A new scene text recognizer with visual language modeling network," in *Proceedings of the IEEE/CVF International Conference on Computer Vision*, 2021, pp. 14 194–14 203.
 [9] S. Fang, H. Xie, Y. Wang, Z. Mao, and Y. Zhang, "Read like humans: Autonomous, bidirectional and iterative language modeling for scene text recognition," in *Proceedings of the IEEE/CVF Conference on Computer Vision and Pattern Recognition*, 2021, pp. 7098–7107.
 [10] B. Na, Y. Kim, and S. Park, "Multi-modal text recognition networks: Interactive enhancements between visual and semantic features," in *European Conference on Computer Vision*. Springer, 2022, pp. 446–463.
 [11] X. Wu, B. Tang, M. Zhao, J. Wang, and Y. Guo, "Str transformer: a cross-domain transformer for scene text recognition," *Applied Intelligence*, vol. 53, no. 3, pp. 3444–3458, 2023.
 [12] D. Bautista and R. Atienza, "Scene text recognition with permuted autoregressive sequence models," in *European Conference on Computer Vision*. Springer, 2022, pp. 178–196.
 [13] S. Zhao, X. Wang, L. Zhu, and Y. Yang, "Clip4str: A simple baseline for scene text recognition with pre-trained vision-language model," *arXiv preprint arXiv:2305.14014*, 2023.
 [14] Z. Qiao, Y. Zhou, D. Yang, Y. Zhou, and W. Wang, "Seed: Semantics enhanced encoder-decoder framework for scene text recognition," in *Proceedings of the IEEE/CVF conference on computer vision and pattern recognition*, 2020, pp. 13 528–13 537.
 [15] N. Nguyen, T. Nguyen, V. Tran, M.-T. Tran, T. D. Ngo, T. H. Nguyen, and M. Hoai, "Dictionary-guided scene text recognition," in *Proceedings of the IEEE/CVF Conference on Computer Vision and Pattern Recognition*, 2021, pp. 7383–7392.
 [16] A. Vaswani, N. Shazeer, N. Parmar, J. Uszkoreit, L. Jones, A. N. Gomez, Ł. Kaiser, and I. Polosukhin, "Attention is all you need," *Advances in neural information processing systems*, vol. 30, 2017.
 [17] J. Long, E. Shelhamer, and T. Darrell, "Fully convolutional networks for semantic segmentation," in *Proceedings of the IEEE conference on computer vision and pattern recognition*, 2015, pp. 3431–3440.
 [18] P. Lyu, M. Liao, C. Yao, W. Wu, and X. Bai, "Mask textspotter: An end-to-end trainable neural network for spotting text with arbitrary shapes," in *Proceedings of the European conference on computer vision (ECCV)*, 2018, pp. 67–83.
 [19] Z. Wan, M. He, H. Chen, X. Bai, and C. Yao, "Textscanner: Reading characters in order for robust scene text recognition," in *Proceedings of the AAAI conference on artificial intelligence*, vol. 34, no. 07, 2020, pp. 12 120–12 127.
 [20] M. Liang and X. Hu, "Recurrent convolutional neural network for object recognition," in *Proceedings of the IEEE conference on computer vision and pattern recognition*, 2015, pp. 3367–3375.

- [21] A. Graves and A. Graves, "Connectionist temporal classification," *Supervised sequence labelling with recurrent neural networks*, pp. 61–93, 2012.
- [22] B. Shi, X. Bai, and C. Yao, "An end-to-end trainable neural network for image-based sequence recognition and its application to scene text recognition," *IEEE transactions on pattern analysis and machine intelligence*, vol. 39, no. 11, pp. 2298–2304, 2016.
- [23] D. Bahdanau, K. Cho, and Y. Bengio, "Neural machine translation by jointly learning to align and translate," *arXiv preprint arXiv:1409.0473*, 2014.
- [24] Z. Cheng, Y. Xu, F. Bai, Y. Niu, S. Pu, and S. Zhou, "Aon: Towards arbitrarily-oriented text recognition," in *Proceedings of the IEEE conference on computer vision and pattern recognition*, 2018, pp. 5571–5579.
- [25] C.-Y. Lee and S. Osindero, "Recursive recurrent nets with attention modeling for ocr in the wild," in *Proceedings of the IEEE conference on computer vision and pattern recognition*, 2016, pp. 2231–2239.
- [26] H. Li, P. Wang, C. Shen, and G. Zhang, "Show, attend and read: A simple and strong baseline for irregular text recognition," in *Proceedings of the AAAI conference on artificial intelligence*, vol. 33, no. 01, 2019, pp. 8610–8617.
- [27] M. Jaderberg, K. Simonyan, A. Vedaldi, and A. Zisserman, "Synthetic data and artificial neural networks for natural scene text recognition," *arXiv preprint arXiv:1406.2227*, 2014.
- [28] A. Dosovitskiy, L. Beyer, A. Kolesnikov, D. Weissenborn, X. Zhai, T. Unterthiner, M. Dehghani, M. Minderer, G. Heigold, S. Gelly *et al.*, "An image is worth 16x16 words: Transformers for image recognition at scale," *arXiv preprint arXiv:2010.11929*, 2020.
- [29] R. Atienza, "Vision transformer for fast and efficient scene text recognition," in *International Conference on Document Analysis and Recognition*. Springer, 2021, pp. 319–334.
- [30] J. Baek, Y. Matsui, and K. Aizawa, "What if we only use real datasets for scene text recognition? toward scene text recognition with fewer labels," in *Proceedings of the IEEE/CVF Conference on Computer Vision and Pattern Recognition*, 2021, pp. 3113–3122.
- [31] L. Wu, Y. Xu, J. Hou, C. L. P. Chen, and C.-L. Liu, "A two-level rectification attention network for scene text recognition," *IEEE Transactions on Multimedia*, vol. 25, pp. 2404–2414, 2023.
- [32] M. Li, B. Fu, H. Chen, J. He, and Y. Qiao, "Dual relation network for scene text recognition," *IEEE Transactions on Multimedia*, vol. 25, pp. 4094–4107, 2023.
- [33] C. Xue, J. Huang, W. Zhang, S. Lu, C. Wang, and S. Bai, "Image-to-character-to-word transformers for accurate scene text recognition," *IEEE Transactions on Pattern Analysis and Machine Intelligence*, 2023.
- [34] S. Xia, J. Kou, N. Liu, and T. Yin, "Scene text recognition based on two-stage attention and multi-branch feature fusion module," *Applied Intelligence*, vol. 53, no. 11, pp. 14 219–14 232, 2023.
- [35] L. Diao, X. Tang, J. Wang, G. Xie, and J. Hu, "Hierarchical visual-semantic interaction for scene text recognition," *Information Fusion*, vol. 102, p. 102080, 2024.
- [36] X. Zhang, B. Zhu, X. Yao, Q. Sun, R. Li, and B. Yu, "Context-based contrastive learning for scene text recognition," in *Proceedings of the AAAI Conference on Artificial Intelligence*, vol. 36, no. 3, 2022, pp. 3353–3361.
- [37] J. Devlin, M.-W. Chang, K. Lee, and K. Toutanova, "Bert: Pre-training of deep bidirectional transformers for language understanding," *arXiv preprint arXiv:1810.04805*, 2018.
- [38] T. Wang, Y. Zhu, L. Jin, C. Luo, X. Chen, Y. Wu, Q. Wang, and M. Cai, "Decoupled attention network for text recognition," in *Proceedings of the AAAI conference on artificial intelligence*, vol. 34, no. 07, 2020, pp. 12 216–12 224.
- [39] A. Radford, J. W. Kim, C. Hallacy, A. Ramesh, G. Goh, S. Agarwal, G. Sastry, A. Askell, P. Mishkin, J. Clark *et al.*, "Learning transferable visual models from natural language supervision," in *International conference on machine learning*. PMLR, 2021, pp. 8748–8763.
- [40] H. Touvron, M. Cord, M. Douze, F. Massa, A. Sablayrolles, and H. Jégou, "Training data-efficient image transformers & distillation through attention," in *International conference on machine learning*. PMLR, 2021, pp. 10 347–10 357.
- [41] Z. Yang, Z. Dai, Y. Yang, J. Carbonell, R. R. Salakhutdinov, and Q. V. Le, "Xlnet: Generalized autoregressive pretraining for language understanding," *Advances in neural information processing systems*, vol. 32, 2019.
- [42] A. Gupta, A. Vedaldi, and A. Zisserman, "Synthetic data for text localisation in natural images," in *Proceedings of the IEEE conference on computer vision and pattern recognition*, 2016, pp. 2315–2324.
- [43] A. Veit, T. Matera, L. Neumann, J. Matas, and S. Belongie, "Coco-text: Dataset and benchmark for text detection and recognition in natural images," *arXiv preprint arXiv:1601.07140*, 2016.
- [44] B. Shi, C. Yao, M. Liao, M. Yang, P. Xu, L. Cui, S. Belongie, S. Lu, and X. Bai, "Icdar2017 competition on reading chinese text in the wild (rctw-17)," in *2017 14th iapr international conference on document analysis and recognition (ICDAR)*, vol. 1. IEEE, 2017, pp. 1429–1434.
- [45] Y. Zhang, L. Gueguen, I. Zharkov, P. Zhang, K. Seifert, and B. Kadlec, "Uber-text: A large-scale dataset for optical character recognition from street-level imagery," in *SUNw: Scene Understanding Workshop-CVPR*, vol. 2017, 2017, p. 5.
- [46] C. K. Chng, Y. Liu, Y. Sun, C. C. Ng, C. Luo, Z. Ni, C. Fang, S. Zhang, J. Han, E. Ding *et al.*, "Icdar2019 robust reading challenge on arbitrary-shaped text-rrc-art," in *2019 International Conference on Document Analysis and Recognition (ICDAR)*. IEEE, 2019, pp. 1571–1576.
- [47] Y. Sun, Z. Ni, C.-K. Chng, Y. Liu, C. Luo, C. C. Ng, J. Han, E. Ding, J. Liu, D. Karatzas *et al.*, "Icdar 2019 competition on large-scale street view text with partial labeling-rrc-lsvt," in *2019 International Conference on Document Analysis and Recognition (ICDAR)*. IEEE, 2019, pp. 1557–1562.
- [48] N. Nayef, Y. Patel, M. Busta, P. N. Chowdhury, D. Karatzas, W. Khelif, J. Matas, U. Pal, J.-C. Burie, C.-I. Liu *et al.*, "Icdar2019 robust reading challenge on multi-lingual scene text detection and recognition—rrc-mlt-2019," in *2019 International conference on document analysis and recognition (ICDAR)*. IEEE, 2019, pp. 1582–1587.
- [49] R. Zhang, Y. Zhou, Q. Jiang, Q. Song, N. Li, K. Zhou, L. Wang, D. Wang, M. Liao, M. Yang *et al.*, "Icdar 2019 robust reading challenge on reading chinese text on signboard," in *2019 international conference on document analysis and recognition (ICDAR)*. IEEE, 2019, pp. 1577–1581.
- [50] A. Singh, G. Pang, M. Toh, J. Huang, W. Galuba, and T. Has-sner, "Textocr: Towards large-scale end-to-end reasoning for arbitrary-shaped scene text," in *Proceedings of the IEEE/CVF conference on computer vision and pattern recognition*, 2021, pp. 8802–8812.
- [51] I. Krylov, S. Nosov, and V. Sovrasov, "Open images v5 text annotation and yet another mask text spotter," in *Asian Conference on Machine Learning*. PMLR, 2021, pp. 379–389.
- [52] A. Mishra, K. Alahari, and C. Jawahar, "Scene text recognition using higher order language priors," in *BMVC-British machine vision conference*. BMVA, 2012.
- [53] A. Risnumawan, P. Shivakumara, C. S. Chan, and C. L. Tan, "A robust arbitrary text detection system for natural scene images," *Expert Systems with Applications*, vol. 41, no. 18, pp. 8027–8048, 2014.
- [54] K. Wang, B. Babenko, and S. Belongie, "End-to-end scene text recognition," in *2011 International conference on computer vision*. IEEE, 2011, pp. 1457–1464.
- [55] T. Q. Phan, P. Shivakumara, S. Tian, and C. L. Tan, "Recognizing text with perspective distortion in natural scenes," in *Proceedings of the IEEE international conference on computer*

- vision, 2013, pp. 569–576.
- [56] D. Karatzas, F. Shafait, S. Uchida, M. Iwamura, L. G. i Bigorda, S. R. Mestre, J. Mas, D. F. Mota, J. A. Almazan, and L. P. De Las Heras, “Icdar 2013 robust reading competition,” in *2013 12th international conference on document analysis and recognition*. IEEE, 2013, pp. 1484–1493.
- [57] D. Karatzas, L. Gomez-Bigorda, A. Nicolaou, S. Ghosh, A. Bagdanov, M. Iwamura, J. Matas, L. Neumann, V. R. Chandrasekhar, S. Lu *et al.*, “Icdar 2015 competition on robust reading,” in *2015 13th international conference on document analysis and recognition (ICDAR)*. IEEE, 2015, pp. 1156–1160.
- [58] M. Li, B. Fu, Z. Zhang, and Y. Qiao, “Character-aware sampling and rectification for scene text recognition,” *IEEE Transactions on Multimedia*, vol. 25, pp. 649–661, 2023.
- [59] A. Paszke, S. Gross, F. Massa, A. Lerer, J. Bradbury, G. Chanan, T. Killeen, Z. Lin, N. Gimeshein, L. Antiga *et al.*, “Pytorch: An imperative style, high-performance deep learning library,” *Advances in neural information processing systems*, vol. 32, 2019.
- [60] G. Lan, “An optimal method for stochastic composite optimization,” *Mathematical Programming*, vol. 133, no. 1-2, pp. 365–397, 2012.
- [61] L. N. Smith and N. Topin, “Super-convergence: Very fast training of neural networks using large learning rates,” in *Artificial intelligence and machine learning for multi-domain operations applications*, vol. 11006. SPIE, 2019, pp. 369–386.
- [62] E. D. Cubuk, B. Zoph, J. Shlens, and Q. V. Le, “Randaug-ment: Practical automated data augmentation with a reduced search space,” in *Proceedings of the IEEE/CVF conference on computer vision and pattern recognition workshops*, 2020, pp. 702–703.